SPE 90904

A New OCTG Strength Equation for Collapse Under Combined Loads

F.J. Klever, Shell International E&P, The Netherlands; and T. Tamano, Kogakuin University, Japan

This paper was prepared for presentation at the SPE Annual Technical Conference and Exhibition held in Houston, Texas, U.S.A., 26–29 September 2004.

Abstract

Wells are becoming more challenging and casing designers are faced with increasing design pressures. Deep hydrocarbon targets lead to requirements for the casing to resist collapse under external pressure while significant internal pressure and axial compression or tension may exist at the same time.

This paper describes the development, and its evaluation, of a new collapse strength equation for oil country tubular goods (OCTG). It is based on a generalization of a model previously proposed by Tamano *et al.*[1]. The new model is evaluated through comparisons with both finite element analyses and test data. It is more accurate in dealing with combined internal pressure, external pressure and axial load than, for example, the model currently provided in API Bulletin 5C3[2].

The joint API/ISO SC5 Work Group 2B tasked with modernizing the API 5C3 property equations has evaluated a number of collapse models available in the literature on their performance against several different collapse databases. As a result the model presented here is recommended for developing collapse ratings in the new ISO 10400 standard.

1. Introduction

The design collapse strength equations currently used in the industry and provided in API Bulletin 5C3[2] give a highly non-uniform failure probability over diameter, weight and grade for downhole well tubulars[3]. In addition, the API 5C3 *average* collapse strength equations are relatively poor predictors of true collapse and hence no compelling case exists to use these equations for qualifying high collapse pipe and other proprietary products. Furthermore, designing deep wells is becoming more challenging due to requirements for the casing to resist collapse under external pressure while significant internal pressure and axial compression or tension may exist at the same time. This highlighted the need for revisiting the method to account for combined loading in collapse.

The situation may be improved if more accurate collapse prediction formulas could be developed that capture adequately the physics of collapse failure, and include more explicitly the effect of imperfections. Because the collapse failure mechanism is an instability phenomenon – i.e. the transition from an essentially round pipe to a pipe that starts to ovalize and flatten with the external pressure capacity reaching a maximum can happen very quickly – it is not feasible to expect a simple equation to capture this failure mechanism very accurately. However, theoretical analyses, detailed finite-element analyses and numerous collapse tests have provided a wealth of insight that has guided the development of approximate collapse equations that capture collapse failure to a satisfactory degree.

Like other currently available models the model presented in this paper consists of a number of interlinked concepts:

a) An equation for *elastic* collapse of a perfect pipe, relevant for very thin pipe
b) An equation for through-wall *yield* collapse of a perfect pipe, relevant for very thick pipe
c) An equation providing a *transition* between elastic collapse and yield collapse, thus predicting the collapse strength for all relevant pipe sizes, weights and grades.
d) Factors to incorporate the effect of *imperfections* such as ovality, stress-strain curve shape, residual stress and eccentricity

An additional objective of this paper is to address the effect of combined loading. API 5C3 describes a conservative method to account for axial load and internal pressure, focused on use with its lower bound design strength equations. However, deriving risk-based collapse ratings require an Ultimate Limit State (ULS) model that more accurately predicts the actual (50-percentile) collapse strength. In particular for heavy-walled pipe, the effect of internal pressure on collapse derived from first principles shows interesting differences with the API 5C3 formulation. For very deep wells the new approach to combined loading can have significant economic implications.

In the following sections, firstly collapse of ideal pipe is addressed, providing formulas for elastic collapse and yield collapse under combined loading (section 2). The new general formula predicting collapse for all relevant pipe sizes, weights and grades and including the effect of imperfections is presented in section 3. Section 4 provides additional observations about the new equation and compares it with some well-known existing equations. Section 5 addresses its performance against finite-element analyses and tests. The paper ends with a number of conclusions.

2. Collapse of an Ideal Pipe

For a perfectly round pipe without further imperfections collapse under external over-pressure constitutes an instability phenomenon. For both elastic and elastic-plastic situations theoretical analyses have lead to closed form solutions for the collapse pressure under combined loads. The underlying shell theory approximation is more accurate for thin-walled pipe and hence only the result for elastic collapse is used.

Finite-element analyses of pipe with *D/t* ranging from 10 to 26 showed that thick-walled pipe collapses when the plastic zone has extended almost entirely through the wall[1]. Hence the through-wall yield pressure may best approximate the yield collapse pressure of thick-walled pipe. This concept allowed for a derivation in closed form of the yield collapse pressure under combined loads that accounts for all three axial, circumferential *and* radial stresses, and thus is more accurate than the method described in API 5C3.

Elastic Collapse

Derived in Appendix A, the elastic collapse pressure difference $p_e - p_i$ under combined loads is described by

$$\Delta p^{ec} = \frac{2E'}{1-\nu^2}\,\xi^3\,(1+c\,\xi) \tag{1}$$

where c is a model constant,

$$\xi = \frac{1}{D_{av}/t_{av} - 1} \tag{2}$$

and the factored Young's modulus is

$$E' = k_e\,(1-H_e)\,E \tag{3}$$

The model bias factor k_e and the decrement function H_e accounting for imperfections will be discussed below in section 3. From classical collapse theory it follows that elastic collapse is only a function of internal and external pressure, and not dependent on axial load.

For $c = 0$ equation (1) reverts to the thin-wall collapse equation found in textbooks. For $c = -1+t/D$ the formula from Clinedinst[4] used in API 5C3 (excluding the bias factor of 0.95) is recovered. However, theoretical considerations[5] require the elastic collapse strength for thick-walled pipe to be higher than that predicted by thin-wall theory, hence $c \geq 0$. This has been confirmed with finite-element analyses (FEA). Fig. 1 shows how c affects the elastic collapse prediction.

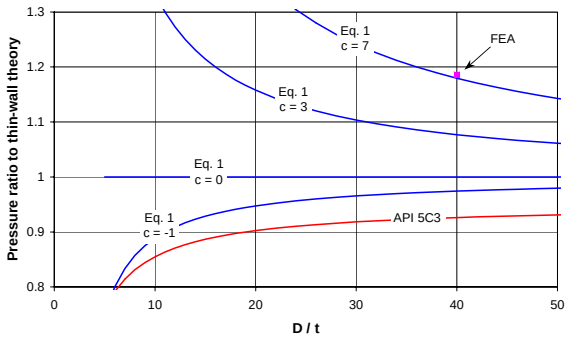

Fig. 1 Comparison of API average elastic collapse, eq. (1) for various values of *c*, and FEA result for a perfect pipe

Yield Collapse

A very thick pipe will yield before it reaches its collapse pressure. For materials with a limited amount of strain hardening there will be little margin between through-wall yielding and actual collapse, hence the term 'yield collapse' used historically. Under the combined action of external pressure, internal pressure and axial load, a closed-form through-wall yield formulation has been developed (see Appendix C) based on a '3D-average' or < 3D > theory (see Appendix B) involving stresses and strains that are uniform over the wall thickness.

The yield collapse pressure difference is described by

$$\Delta p^{yc} = \min\left\{\frac{1}{2}\left(\Delta p^{yM} + 2\xi\,\sigma'_y\right)\ ,\ \Delta p^{yM}\right\} \tag{4}$$

where the yield pressure according to the von Mises criterion

$$\Delta p^{yM} = \xi\,\sigma'_y\,\frac{4(1+2\xi)}{3+(1+2\xi)^2}\left[-S_i \pm \sqrt{1+3\,\frac{1-S_i^2}{(1+2\xi)^2}}\right] \tag{5}$$

Equation (4) yields the average of the Tresca and von Mises collapse pressure predictions in the axial compression range. Equation (5) describes all four quadrants of the von Mises through-wall yield envelope, but the plus sign is relevant for almost all of the practical collapse situations where, naturally, $\Delta p > 0$. Axial load and internal pressure are incorporated:

$$S_i = \frac{\sigma_a + p_i}{\sigma'_y} \tag{6}$$

The factored yield strength is

$$\sigma'_y = k_y\,(1-H_y)\,\sigma_y \tag{7}$$

The model bias factor k_y and the decrement function H_y accounting for imperfections will be discussed in section 3.

Equation (5) is accurate to order ξ^2 and is, as Fig. 2 shows, very accurate indeed when compared with the exact through-wall von Mises yield pressure obtained by solving the exact equations with an extremely accurate numerical scheme.

Also shown in Fig. 2 are two FEA results for collapse of very thick-walled pipes where the material model included the work hardening of actual L80 material (yield strength = 89.7 ksi, ultimate strength = 105 ksi). Clearly for the $D/t = 8$ case the pipe collapsed beyond yield in the work hardening range; for $D/t = 10$ collapse occurred at through-wall yield.

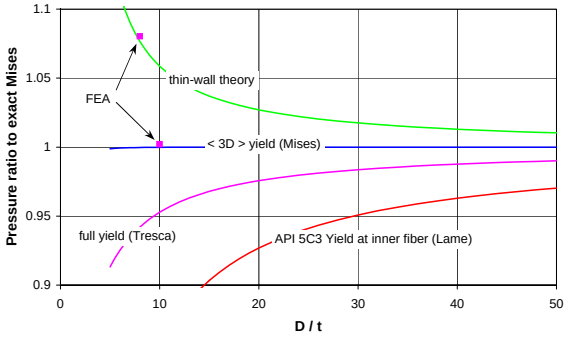

Fig. 2 Comparison of API yield collapse, Tresca yield, eq. (4), thin-walled yield, and FEA results (perfect pipe; $S_i = 0$)

3. New OCTG Collapse Equation

Inspired by the approach presented by Tamano *et al.*[1] a transition between the models for yield collapse for very thick pipe and elastic collapse for very thin pipe is proposed comprising the following quadratic form:

$$\Delta p^{c} = \frac{2\ \Delta p^{yc}\ \Delta p^{ec}}{\Delta p^{yc} + \Delta p^{ec} + \sqrt{\left(\Delta p^{yc} - \Delta p^{ec}\right)^2 + 4\,H_t\ \Delta p^{yc}\ \Delta p^{ec}}} \quad (8)$$

The yield collapse and elastic collapse pressures are given by equations (4) and (1), respectively. The decrement function H_t is having its maximum effect at the transition point, i.e. the combination of yield strength and *D/t* ratio where the yield collapse pressure Δp^{yc} equals the elastic collapse pressure Δp^{ec}.

For thick-walled pipe $\Delta p^{ec} >> \Delta p^{yc}$ and equation (8) converges to $\Delta p^{c} \cong \Delta p^{yc}$, whereas for thin-walled pipe $\Delta p^{ec} << \Delta p^{yc}$ and $\Delta p^{c} \cong \Delta p^{ec}$. Note also that for $H_t = 0$ the collapse pressure Δp^{c} is simply the smaller of Δp^{yc} and Δp^{ec}.

Accounting for Imperfections

The models for elastic collapse and yield collapse are based on first principles, but they have been derived for ideal pipes. Collapse strength, however, is negatively influenced by imperfections such as ovality, shape of the material stress-strain curve, eccentricity and residual stress.

Decrement Functions

Purely elastic collapse is a stable process (the pressure does not decrease under continued ovalization) but for realistic well tubulars even pipes that start collapse in the elastic range will soon develop plasticity at the inner fibers and hence show a clear pressure maximum. This means that ovality impacts the collapse strength of all well tubulars, thick-walled and thin-walled.

The effect of imperfections has been incorporated in the model by means of the empirical functions H_y, H_t and H_e that de-rate the strengths in the yield region, the transition region and the elastic region, respectively. These decrement functions may be taken in an additive form:

$$H_j = H_j^{ov}(ov,\xi) + H_j^{ec}(ec,\xi) + H_j^{rs}(rs,\xi) + H_j^{sh}(sh,\xi) \quad (9)$$

where the subscript *j* denotes either *y*, *t* or *e*. Note, however, that there is, for example, a strong interaction between stress-strain curve shape and sensitivity to ovality[6], so for non-quenched and tempered materials or cold worked materials the decrement contributions H^{ov} and H^{sh} may better be combined.

In their simplest form the decrement functions may be taken independent of ξ and linearly in the imperfections *ov*, *ec*, *rs* and *sh*. API/ISO SC5 WG2B has taken that initial approach and yet has shown that the above model with only H_t, and vanishing H_y and H_e, outperformed other collapse models available from the literature when evaluated against the WG2B collapse test database.

Timoshenko[7] determined at which external pressure a thin-walled pipe with an initial ovality reaches the yield stress at the extreme fibers. This analysis is lower bound to the collapse pressure, and it leads to a decrement function that is linear in *ov* and inversely proportional to ξ.

Finite-element analyses[8] has been used to identify the functional relationships of the decrement functions in some more detail. For a given grade, the decrease of collapse strength due to ovality is much stronger in the transition region than for pipes that are either very thick-walled or thin-walled. This can be modeled by taking different (though maybe still linear in *ov*) functions H_y^{ov}, H_t^{ov} and H_e^{ov}.

The effect of eccentricity seems independent from *D/t* ratio and symmetric in *ec*. This can be established in the model by taking $H_y^{ec} = H_e^{ec}$ proportional to ec^2 and $H_t^{ec} = 0$.

The effect of residual stress may be considered symmetric in *rs* and is more pronounced in the transition region than in the elastic region. Collapse pressures for tubulars with very low *D/t* ratio are largely unaffected by residual stress. Taking different functions H_y^{rs}, H_t^{rs} and H_e^{rs} that are quadratic, or even quartic, in *rs* may approximate this.

Finally, the effect of stress-strain curve shape can be very significant. If the proportional limit of the material is much lower than the yield strength (the stress reached at 0.5% total strain) the stiffness above the proportional stress reduces below the Young's modulus and this in turn decreases the collapse strength. Pipes that have undergone cold working, for instance due to cold straightening or due to diametrical expansion, will generally show this effect, quite possibly reducing the collapse strength by up to tenths of percent.

Bias Factors

For any given approach to accounting for imperfections through decrement functions, the factors k_y and k_e can be used to adjust the model predictions by a fixed factor. In this way the model can be biased such that it matches the average of a particular collapse test database, thus leading to factors $k_{y\,uls}$ and $k_{e\,uls}$ that provide the best prediction of the *average* collapse strength.

In addition, k_y and k_e may be used to develop an equation that approximates a characteristic value (say the 0.5-percentile) of the collapse strength probability distribution. In that case factors $k_{y\,des}$ and $k_{e\,des}$ establish the margin to the *design* collapse strength associated with the desired target reliability level.

4. Further Analysis of the New Equation

Defining dimensionless collapse pressures *Y* or *XY* and a dimensionless "data space" variable *X* as

$$Y = \frac{\Delta p^{c}}{\Delta p^{yc}} \ ; \ XY = \frac{\Delta p^{c}}{\Delta p^{ec}} \ ; \ X = \frac{\Delta p^{yc}}{\Delta p^{ec}} \quad (10)$$

equation (8) is the solution of the following quadratic form:

$$\left(1 - H_t\right) X Y^2 - \left(1 + X\right) Y + 1 = 0 \quad (11)$$

Here the focus is on the ratio *Y* of collapse pressure over *yield* collapse pressure. Alternatively, the ratio *XY* of collapse pressure over *elastic* collapse pressure may be considered and then equation (8) or equation (11) may be written as

$$\left(1 - H_t\right) \frac{1}{X} (XY)^2 - \left(1 + \frac{1}{X}\right)(XY) + 1 = 0 \quad (12)$$

In the limit of very thick-walled pipe $X \to 0$ and $Y \to 1$ and the solution converges to yield collapse, equation (4). For very thin-walled pipe $1/X \to 0$ and $XY \to 1$ and the solution

converges to elastic collapse, equation (1). At the transition point where $X = 1$ the solution is $Y = XY = 1/(1+\sqrt{H_t})$.

Comparing (11) and (12) it is clear that Y as a function of X behaves entirely similar to XY as a function of $1/X$. Hence by defining

$$\Delta p^{ref} = \min\left\{\Delta p^{yc}, \Delta p^{ec}\right\} \quad (13)$$

the ratio of Δp^{c} over Δp^{ref} is a symmetrical function of $\log(X)$ as shown in Fig. 3.

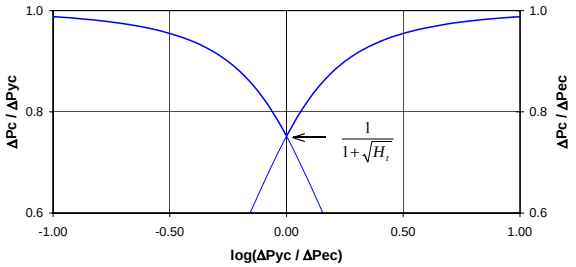

Fig. 3 Collapse pressure difference as a function of log(*X*)

In order to compare the new collapse equation with other equations published in the literature, plots are generated using the uniaxial version of Δp^{ref}

$$p^{ref} = 2\xi \min\left\{\sigma_y(1-0.5\xi), \frac{E}{1-\nu^2}\xi^2(1+c\xi)\right\} \quad (14)$$

Timoshenko Model

The Timoshenko model[7] of a thin-walled pipe with an initial ovality *ov* reaching yield at the extreme fibers due to (only) external pressure p_e can be expressed as

$$\chi\gamma^2 - \left(1 + a\sqrt{\chi} + \chi\right)\gamma + 1 = 0 \quad (15)$$

where

$$\gamma = \frac{p_e^c}{p_{thin}^{yc}} \quad ; \quad \chi\gamma = \frac{p_e^c}{p_{thin}^{ec}} \quad ; \quad \chi = \frac{p_{thin}^{yc}}{p_{thin}^{ec}} \quad (16)$$

where the (uniaxial, thin-walled) yield pressure and the elastic collapse pressure are, respectively,

$$p_{thin}^{yc} = 2\xi\sigma_y \quad (17)$$

$$p_{thin}^{ec} = \frac{2E}{(1-\nu^2)}\xi^3 \quad (18)$$

Hence

$$\chi = \frac{p_{thin}^{yc}}{p_{thin}^{ec}} = (1-\nu^2)\frac{\sigma_y}{E}\frac{1}{\xi^2} = (1-\nu^2)\frac{\sigma_y}{E}\left(\frac{D}{t}-1\right)^2 \quad (19)$$

In the Timoshenko equation the effect of ovality *ov* has been explicitly modeled and found as

$$a = \frac{3\,ov}{2\sqrt{(1-\nu^2)\sigma_y/E}} \quad ; \quad a\sqrt{\chi} = \frac{3}{2}ov\left(\frac{D}{t}-1\right) \quad (20)$$

In the limit of thick-walled pipe $\chi \to 0$ and $\gamma \to 1$ and the solution converges to yield collapse, equation (17). For very thin-walled pipe $1/\chi \to 0$ and $\chi\gamma \to 1$ and the solution converges to elastic collapse, equation (18). At the transition point where $\chi = 1$ the solution is $\gamma = \chi\gamma = 1+a/2-\sqrt{(a(1+a/4))}$.

Note that from Timoshenko's analysis follows that the effect of ovality is maximum in the transition range, and is fading out to zero for either very thick-walled or very thin-walled pipes.

Tamano Model

The Tamano model[1] of a pipe loaded by external pressure and axial load can be expressed as

$$x\,y^2 - (1+x)y + 1 - H = 0 \quad (21)$$

with the decrement function H proposed as a linear function of imperfections such as ovality, eccentricity and residual stress. In equation (21)

$$y = \frac{p_e^c}{p_e^{ycT}} \quad ; \quad xy = \frac{p_e^c}{p_e^{ecT}} \quad ; \quad x = \frac{p_e^{ycT}}{p_e^{ecT}} \quad (22)$$

where the yield pressure and the elastic collapse pressure were, respectively,

$$p_e^{ycT} = 2\sigma_y \frac{D/t-1}{(D/t)^2}\left(1+\frac{fac}{D/t-1}\right)\left[\sqrt{1-\frac{3}{4}\left(\frac{\sigma_a}{\sigma_y}\right)^2} - \frac{1}{2}\frac{\sigma_a}{\sigma_y}\right] \quad (23)$$

$$p_e^{ecT} = \frac{2E}{1-\nu^2}\frac{1}{D/t(D/t-1)^2} \quad (24)$$

Based on curve-fitting the results of elastic-plastic finite-element analyses Tamano *et al.*[1] proposed $fac = 1.47$. However, it can be shown (see Appendix C) that taking $fac = 1.5$ leads to a through-wall yield collapse pressure formula that is second order correct in t/D and in that case equation (23) simplifies to

$$p_e^{ycT} = 2\sigma_y \frac{t}{D}\left(1+\frac{1}{2}\frac{t}{D}\right)\left[\sqrt{1-\frac{3}{4}\left(\frac{\sigma_a}{\sigma_y}\right)^2} - \frac{1}{2}\frac{\sigma_a}{\sigma_y}\right] \quad (25)$$

In the limit of very thick-walled pipe $x \to 0$ and $y \to 1-H$ and the solution converges to a factored value of the yield collapse pressure, equation (25). For very thin-walled pipe $1/x \to 0$ and $xy \to 1-H$ and the solution converges to a factored value of elastic collapse pressure, equation (24). At the transition point where $x = 1$ the solution is $y = xy = 1-\sqrt{H}$.

What are the Differences between the Models

Comparing the new collapse model presented in this paper, equation (11), the classical Timoshenko model, equation (15), and the original Tamano model, equation (21), it is clear that all these models comprise a simple quadratic form as a transition between yield collapse and elastic collapse. The differences are found in the way the detrimental effect of imperfections such as ovality is incorporated.

Comparing in particular the original Tamano model[1] with the new model presented in this paper the following differences may be noted:

- The formula for elastic collapse under combined loads, equation (1), is the classical formula augmented with a factor to account for thick-wall effects.
- The formula for yield collapse, equation (4), is second order correct in *t/D* and includes the effect of combined axial load, external pressure *and* internal pressure.
- In the axial compression range the formula for yield collapse takes the average of the von Mises and Tresca yield predictions whenever this is more conservative than the pressure following from the von Mises criterion alone.
- The new collapse strength equation (8) providing the transition between yield collapse and elastic collapse is formulated in terms of the pressure *difference*.
- Yield collapse, transition collapse and elastic collapse each has its separate decrement function to account for the effect of imperfections.
- For yield collapse and elastic collapse the decrement functions are incorporated as "partial resistance factors".

Essentially the collapse equation (8) is general enough to contain many of the earlier published equations, allowing a significantly more flexible tuning to actual test data.

5. Performance of the New Equation

The OCTG collapse equation (8) builds on two components – (a) through-wall yield and (b) elastic collapse of a perfect pipe under combined loads – that have been derived from first principles. The transition between these two components, modeling the collapse strength of real pipe of all sizes, weights and grades is entirely empirical, although Timoshenko's analysis[7] demonstrates that the quadratic form chosen for this transition may be a natural one. The decrement functions H_y, H_t and H_e in equations (3), (7) and (8) allow a comprehensive treatment of the effect of imperfections.

In order to assess the performance of the new model it has been (a) validated with FEA analyses of perfect pipe, (b) compared with other models, and (c) evaluated against tests.

Comparison with FEA

Using an actually measured stress-strain curve of an L80 grade material (see Fig. 4), for three pipe geometries, three levels of internal pressure and two axial load situations finite-element analyses (FEA) have been performed to calculate the collapse pressure. The pipes were essentially perfect, with no initial ovality or eccentricity. Two diametrically opposed very small forces triggered the ovalization deformation associated with the collapse phenomenon. The maximum external pressure recorded during the analysis was taken as the collapse pressure.

The two very low *D/t* ratios were chosen to validate the yield collapse formula (4); the $D/t = 40$ case collapses in the elastic range and served to verify equation (1). Three levels of internal pressure were chosen, and in each case the internal pressure was applied first and kept fixed, with the external pressure incrementally (using an arc length continuation method) applied until a maximum was identified. Finally, these sets of analyses have been performed for the situation of axial plane strain (zero axial strain) and axial plane stress (zero axial load).

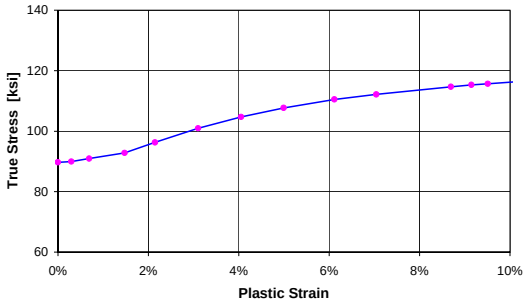

Fig. 4 Actual L80 stress-strain curve

The results are summarized in Table 1 in terms of the pressure difference $p_e - p_i$ at collapse.

Table 1 FEA results for collapse pressure Δp^c of a perfect pipe under various axial load and internal pressure situations (realistic L80 stress-strain curve, $p_y = 2\xi\sigma_y$ and σ_y = 89.7 ksi)

D/t		Axial Plane Strain			Zero Axial Load		
8	p_i / p_y	0.000	0.435	0.870	0.000	0.438	0.875
	$\Delta p^c / p_y$	1.108	1.101	1.094	1.003	1.004	0.987
10	p_i / p_y	0.000	0.450	0.900	0.000	0.450	0.900
	$\Delta p^c / p_y$	1.077	1.072	1.066	0.947	0.898	0.850
40	p_i / p_y	0.000	0.488	0.975	0.000	0.488	0.975
	$\Delta p^c / p_y$	0.283	0.283	0.283	0.283	0.283	0.283

The FEA results listed in Table 1 are also shown in Fig. 5, together with the predictions of equation (8) given by the blue curves. Note that in Fig. 5 the stresses have been calculated from the loads using the < 3D > equilibrium equations (B-12).

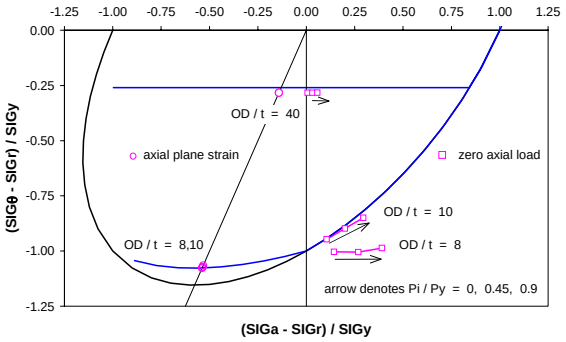

Fig. 5 Collapse of perfect pipes: FEA results compared with eq. (8) where $H_y = H_t = H_e = 0$, $k_y = k_e = 1$ and $c = 3$

For the axial plane strain case the FEA results are only dependent on the pressure *difference*, just as equation (8) predicts. Given a plane strain situation not only elastic collapse but also yield collapse can be shown to be only a function of the pressure difference.

However, for axial load conditions other than plane strain the effect of internal pressure on yield collapse is more involved and is a function of the axial load. This is confirmed by the FEA for zero axial load. Fig. 5 shows the new model (8) with $c = 3$ to fit the elastic FEA for $D/t = 40$ rather well. For $D/t = 8$ the FEA for zero axial load predicts collapse strengths beyond

the through-wall yield envelope, and this is due to the work hardening of the material that was modeled. Equation (8), however, does not account for work hardening and therefore the results for $D/t = 8$ and $D/t = 10$ are essentially equal: the model predicts yield collapse.

For this validation with FEA of perfect pipe, the new equation (8) was used with vanishing decrement functions and with bias factors equal to one, because that is consistent with the FEA for ideal pipe. The effect of work hardening may be approximated by taking the bias factor k_y greater than one, or including a *negative* decrement term in H_y. In that way equation (8) would predict collapse pressures outside the yield envelope, thus possibly improving the model performance for very thick-walled pipe like the $D/t = 8$ case in Fig. 5.

For the axial plane strain case the FEA model for very thick-walled pipe predicted collapse pressures lower than predicted by the von Mises yield criterion. In this axial compression range the new model (8) is based on the average of the predictions using von Mises and Tresca (see eq. (4)) and this appeared to fit the FEA predictions well.

Comparison with Tests

The API/ISO Work Group 2 - as part of their task of modernizing API Bulletin 5C3 / ISO 10400 - evaluated a number of collapse strength prediction models on their performance against an extensive collapse dataset. The data ensemble is in the public domain and contains some 3000 tests comprising both API and high collapse grades from various sources.

Initially a modified version of the Tamano equation was found to predict these tests rather well (see Adams *et al.*[3]). Later, the model presented in this paper appeared to improve upon that predictive accuracy considerably. In fact, this performance was achieved with a simplified version of equation (8), where decrement functions H_y and H_e were taken as zero, and only the transition decrement function H_t was used as a linear function of the ovality, eccentricity and residual stress.

This would suggest that opportunities for further improvement still exist within the framework of the general model presented here, for example by utilizing separate decrement functions in the yield range, the transition range and the elastic range.

Effect of Material Strain Hardening

The two basic components of the collapse model are elastic collapse and through-wall yield collapse. The effect of work hardening of the material has not been taken into account in equation (8) explicitly, and the model is therefore conservative in this respect. Bi-axial collapse tests with K55 pipe shown in Fig. 6 demonstrate that for a hardening material under high axial tension or compression collapse may occur at stresses considerably above yield.

The elastic-plastic collapse model presented in Appendix A has been used to (try to) predict these bi-axial collapse tests. Equation (A-5) has been derived for perfect pipes and should be expected to over-predict actual tests, but it appears that this elastic-plastic thin-walled model captures the behavior reasonably well. There are two tests in the transition range between yield collapse and elastic collapse and for these tests the over-prediction of the simple shell theory model is indeed very significant.

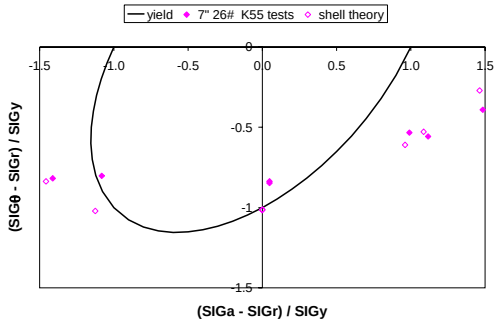

Fig. 6 Biaxial collapse data and predictions by the elastic-plastic shell theory model for perfect pipes eq. (A-5)

Further work to incorporate the effect of work hardening under combined loading into collapse strength prediction formulas would be valuable, perhaps building upon a simplified (but effective) method for a thin-walled collapse formula that has been suggested by Ju *et al.*[8].

Comparison with Other Models

The decrement functions H_y, H_t and H_e in equations (3), (7) and (8) allow a comprehensive, albeit empirical, treatment of the effect of imperfections. For the case of external-pressure-only (and taking $c \cong -1$) the original Tamano[1] formula (21) is recovered when $H_y = H_t = H_e$. The Timoshenko equation (15) can be recovered in several ways, for example by taking

$$1 - H_y = \sqrt{1 - H_t} = 1 - H_e = \frac{1 + \chi}{1 + \chi + a\sqrt{\chi}} \qquad (26)$$

Fig. 7 shows the behavior of a number of formulas, including Timoshenko equation (15), Tamano equation 21 and the API 5C3[2] *average* collapse formulas that are given in Appendix D. A common feature of these models is the dip in the transition range where the effect of imperfections and the decrement function is maximum. The dip level can be set with the decrement values, but the difference between the formulas that remains is in the "dip shape", its slope, convergence to the yield collapse or elastic collapse values, etc. In Fig. 7 only a simplified version of the collapse equation (8) is shown where $k_y = 0.99$, $k_e = 1.09$, $c = -1$, $H_y = H_e = 0$ and $H_t = 0.109$. Introducing non-trivial values for H_y and H_e and/or specific model parameters enables further development of forms of the collapse equation (8) that are specific for particular products.

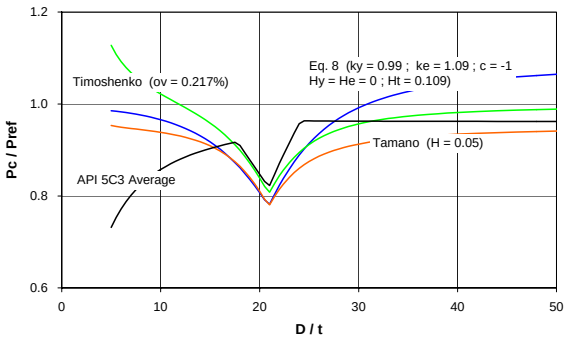

Fig. 7 Comparison of the various models, including a particular simple choice for eq. (8) (grade L80)

Effect of Internal Pressure

An important difference between the collapse strength model presented here and the API 5C3 equations is in the approach towards internal pressure. The API 5C3 Bulletin recommends accounting for internal pressure by defining an "external pressure equivalent" of external pressure and internal pressure. This API 5C3 method is an ad-hoc, but conservative way of dealing with internal pressure in collapse.

In this paper a model has been presented that takes the internal pressure explicitly, and accurately, into account for both the elastic collapse formula and the yield collapse formula. Elastic collapse is purely a function of the pressure *difference*. For yield collapse the < 3D > model showed that the influence of internal pressure on the collapse strength is a function of the axial load.

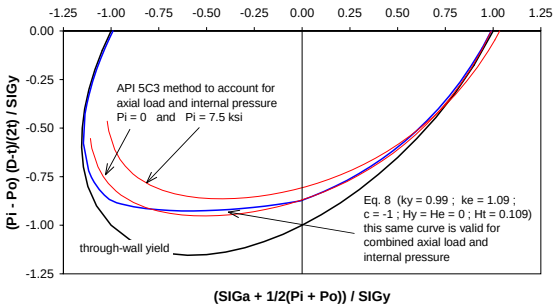

Fig. 8 Effect of internal pressure on the collapse strength predicted by eq. (8), or according to the API 5C3 approach to combined loads eq. (C-19) (7" 29# L80 pipe)

In Fig. 8 an example is given of the predictions by equation (8). When a plot is made using these particular axes parameters the (blue) collapse prediction curve is valid for combined loads; i.e. the curves for different levels of internal pressure coincide.

Note that in Fig. 8 the stress differences commonly plotted along the axes have been expressed in terms of loads using the < 3D > equilibrium equations (B-12):

$$\sigma_\alpha - \sigma_r = \sigma_\alpha + \frac{1}{2}(p_i + p_e) \tag{27}$$

$$\sigma_\theta - \sigma_r = \frac{R}{t}(p_i - p_e) = \frac{D-t}{2t}(p_i - p_e) \tag{28}$$

The other two (red) curves in Fig. 8 demonstrate the difference with the API 5C3 approach to combined loading given by equation (C-19). Both methods give exactly the same collapse pressure for the case of zero axial load and zero internal pressure. However, the API 5C3 method to account for combined loading is not first order correct in *t/D*. The associated differences of up to 10% may have significant economic implications, especially for deep wells.

Conclusions

- A new OCTG collapse strength equation has been presented that the API/ISO Work Group 2 - as part of their task of modernizing API Bulletin 5C3 / ISO 10400 – has found to outperform a number of publicly available collapse strength prediction models when evaluated against an extensive collapse dataset.
- The model comprises a simple, but flexible, quadratic form to interpolate between yield and elastic collapse.
- Both the yield collapse and the elastic collapse components of the new model have been derived from first principles to incorporate the effect of combined axial load *and* internal pressure accurate to second order in *t/D*.
- The effect of imperfections has been accounted for by separate decrement functions in the yield range, the transition range and the elastic range.
- The model may be tuned to various pipe product types and thus form the basis for developing reliability-based design collapse strengths.

Acknowledgments

The authors wish to thank Shell International Exploration and Production and the Kogakuin University for supporting the release of this work.

Nomenclature

c = constant in the elastic collapse equation (1)
D = pipe outside diameter
D_{av} = cross-section-average outside diameter
ec = $(t_{max} - t_{min}) / t_{av}$ = eccentricity
E = Young's modulus
E' = factored Young's modulus, eq. (3)
H_e = decrement factor for elastic collapse, eq. (3)
H_t = decrement factor in transition region, eq. (8)
H_y = decrement factor for yield collapse, eq. (7)
k_e = bias factor for elastic collapse, eq. (3)
k_y = bias factor for yield collapse, eq. (7)
ov = $(D_{max} - D_{min}) / D_{av}$ = ovality
p_e = external pressure
p_i = internal pressure
p^{ref} = reference collapse pressure of ideal pipe, eq. (14)
rs = σ_{res} / σ_y = residual stress over yield stress (compression at the inside diameter is negative)
R = $(D - t) / 2$ = pipe mid-wall radius
sh = parameter characterizing stress-strain curve shape
S_i = combined loading parameter in yield collapse
t = pipe wall thickness
t_{av} = cross-section-average wall thickness
T = τ / σ_y = torsional shear stress over yield stress
X = yield pressure over elastic pressure, eq. (10)
XY = pressure over elastic collapse pressure, eq. (10)
Y = pressure over yield collapse pressure, eq. (10)
Δp = $p_e - p_i$ = pressure difference
Δp^c = collapse pressure difference, eq. (8)
Δp^{ec} = elastic collapse pressure difference, eq. (1)
Δp^{yc} = yield collapse pressure difference, eq. (4)
ν = Poisson's ratio
ξ = $t / (2\,R)$ = characteristic pipe geometry parameter
σ = equivalent stress
σ_a = average axial stress
σ_θ = circumferential, or hoop, stress
σ_r = radial stress
σ_y = yield stress
σ'_y = factored yield stress, eq. (7)
τ = torsional shear stress

References

1. Tamano, T., Mimaki, T. and Yanagimoto, S., "A new empirical formula for collapse resistance of commercial casing", Proc. 2nd Int. OMAES, 1983, pp. 489-495
2. "Bulletin on formulas and calculations for casing, tubing, drill pipe and line pipe properties", API Bulletin 5C3, 6th edition, October 1994
3. Adams, A.J., Moore, P.W. and Payne, M.L., "On the calibration of design collapse strengths for quenched and tempered pipe", paper SPE 85112, Drilling and Completion, Sept. 2003
4. Clinedinst, W.O., "A rational expression for the critical collapsing pressure of pipe under external pressure", Drilling and Production Practice, API, 1939, pp. 383-391
5. Triantafyllidis, N. and Kwon, Y.J., "Thickness effects on the stability of thin walled structures", J. Mech. Phys. Solids, V. 35, 1987, pp. 643-674
6. Kyriakides, S. and Yeh, M.K., "Factors affecting pipe collapse", Engineering Mechanics Research Report 85/1, Dep. of Aerospace Engineering and Engineering Mechanics, The University of Texas at Austin, 1985
7. Timoshenko, S., "*Theory of elastic stability*", first edition, McGraw-Hill (1936), pp. 222-224
8. Ju, G.T., Power, T.L. and Tallin, A.G., "A reliability approach to the design of OCTG tubulars against collapse", paper SPE 48332 presented at the SPE Applied Technology Workshop on Risk Based Design of Well Casing and Tubing, The Woodlands, Texas, USA, May 7-9, 1998
9. Needleman, A. and Tvergaard, V., "Necking of biaxially stretched elastic-plastic circular plates", J. Mech. Phys. Solids, V. 25, 1977, pp. 159-183
10. Pattillo, P.D. and Huang, N.C., "The effect of axial load on casing collapse", paper SPE 9327 presented at the 55th Annual Fall Technical Conference and Exhibition, Dallas, Texas, USA, Sept. 21-24, 1980

Appendix A: Elastic-Plastic Collapse

For convenience the thin-wall theory formulas for elastic-plastic collapse are provided. These can be found in the literature[9,10].

Writing the constitutive equations as

$$\dot{\sigma}_\alpha \;=\; L_{\alpha\beta}\;\dot{\varepsilon}_\beta \tag{A-1}$$

where $L_{\alpha\beta}$ are the elastic-plastic, plane stress stiffness moduli, which are the inverse of the compliance moduli $C_{\alpha\beta}$

$$\begin{aligned} C_{xx} &= \frac{1}{E} + \left(\frac{1}{E_t} - \frac{1}{E}\right)\left[1 - \frac{3}{4}\left(\frac{\sigma_\theta}{\sigma}\right)^2\right] \\ C_{\theta\theta} &= \frac{1}{E} + \left(\frac{1}{E_t} - \frac{1}{E}\right)\left[1 - \frac{3}{4}\left(\frac{\sigma_x}{\sigma}\right)^2\right] \\ C_{x\theta} &= C_{\theta x} = -\frac{\nu}{E} - \left(\frac{1}{E_t} - \frac{1}{E}\right)\left[\frac{1}{2} - \frac{3}{4}\frac{\sigma_x\,\sigma_\theta}{\sigma^2}\right] \end{aligned} \tag{A-2}$$

and where E_t is the slope of the uniaxial stress-strain curve ($\dot{\sigma} = E_t\;\dot{\varepsilon}$), the elastic-plastic, plane stress stiffness modulus in circumferential direction is

$$L_{\theta\theta} \;=\; \frac{C_{xx}}{C_{xx}\,C_{\theta\theta} - C_{x\theta}\,C_{\theta x}} \tag{A-3}$$

For realistic results, it is recommended to use "J_2 deformation theory plasticity" for calculating the moduli in the collapse analysis, replacing E and ν in equation (A-2) by E_s and ν_s respectively

$$E_s \;=\; \frac{\sigma}{\varepsilon} \quad ; \quad \nu_s \;=\; \frac{E_s}{E}\,\nu + \frac{1}{2}\left(1 - \frac{E_s}{E}\right) \tag{A-4}$$

From a bifurcation analysis of a cylinder under axial load and with the internal and external pressure modeled as follower forces, the result for the collapse pressure is

$$\Delta p^c \;=\; p_e - p_i \;=\; \frac{1}{4}\left(\frac{t}{R}\right)^3 L_{\theta\theta} \;=\; 2\,\xi^3\,L_{\theta\theta} \tag{A-5}$$

Elastic Collapse

Note that the thin-wall shell theory equilibrium equations (see e.g. Appendix B) determine the stresses, the stresses determine the moduli, hence the modulus $L_{\theta\theta}$ is, in general, a function of the loading. However, in the elastic range

$$L_{\theta\theta} \;=\; \frac{E}{1-\nu^2} \tag{A-6}$$

and in that case the collapse pressure following from thin-wall theory is not dependent on the axial load.

For thick-walled pipes the elastic collapse strength should be expected[5] above that predicted by thin-wall theory, the more so the thicker the pipe. This may be approximated by adding a multiplicative factor to equation (A-5) that is linear in ξ:

$$\Delta p^c \;=\; p_e \;-\; p_i \;=\; \frac{2\,E}{1-\nu^2}\;\xi^3\;\left(1 + \;c\,\xi\right) \tag{A-7}$$

Appendix B: < 3D > Pipe Equilibrium Equations

For a pipe length with mid-radius R, wall thickness t, that is fixed at one end and loaded with axial load F and torsional moment M at the other end $x = L$, and further loaded with internal pressure p_i and external pressure p_e, the exact equilibrium equations can be conveniently stated in form of the principle of virtual work

$$\delta W_{\text{int}} \;=\; \delta W_{ext} \tag{B-1}$$

Using axial coordinate x, circumferential coordinate θ and radial coordinate r, normal stresses σ_j, normal strains ε_j, displacements u_j, torsional shear stress τ and shear strain γ (no other shear components are considered) and end-section rotation ϕ the internal virtual work is

$$\delta W_{\text{int}} = 2\pi \int_0^L \int_{-t/2}^{+t/2} \left[\sigma_a\;\delta\varepsilon_a \;+\; \sigma_\theta\;\delta\varepsilon_\theta \;+\; \sigma_r\;\delta\varepsilon_r \;+\; \tau\,\delta\gamma\right] r\,dz\;dx \tag{B-2}$$

where the distance from the mid-surface $z = r - R$.

The external virtual work is

$$\delta W_{ext} = 2\pi L\left[\left(p_i\;r\;\delta u_r\right)\Big|_{z=-\frac{t}{2}} - \left(p_e\;r\;\delta u_r\right)\Big|_{z=+\frac{t}{2}}\right] + F\;\delta u_x\Big|_{x=L} + M\;\delta\phi\Big|_{x=L} \tag{B-3}$$

where

$$\dot{u}_\theta\big|_{x=L} = r\,\dot{\phi} = (R+z)\,\dot{\phi} \tag{B-4}$$

For arbitrary kinematically admissible virtual displacements, and using the incremental compatibility equations

$$\dot{\varepsilon}_a = \frac{\partial \dot{u}_x}{\partial x} \;\;;\;\; \dot{\varepsilon}_\theta = \frac{\dot{u}_r}{r} \;\;;\;\; \dot{\varepsilon}_r = \frac{\partial \dot{u}_r}{\partial r} \;\;;\;\; \dot{\gamma} = \frac{\partial \dot{u}_\theta}{\partial x} \tag{B-5}$$

equation (B-1), using (B-2) and (B-3), generates the usual set of axisymmetric pipe equilibrium equations.

In order to develop a model that is correct up to a particular order in $\xi = t/(2R)$ all variables are expanded like

$$f(r) = {}^0f + \frac{z}{R}\,{}^1f + \left(\frac{z}{R}\right)^2 {}^2f + \ldots.. \tag{B-6}$$

For example, after expanding the displacements, (B-5) yields

$$\begin{aligned}
\dot{\varepsilon}_a &= \frac{\partial\,{}^0\dot{u}_x}{\partial x} \\
\dot{\varepsilon}_\theta &= \frac{1}{R}\left[{}^0\dot{u}_r + \frac{z}{R}\left({}^1\dot{u}_r - {}^0\dot{u}_r\right) + \ldots..\right] \\
\dot{\varepsilon}_r &= \frac{1}{R}\left[{}^1\dot{u}_r + 2\frac{z}{R}\,{}^2\dot{u}_r + \ldots..\right] \\
\dot{\phi}\frac{r}{L} &= \dot{\gamma} = \frac{\partial\,{}^0\dot{u}_\theta}{\partial x} + \frac{z}{R}\frac{\partial\,{}^1\dot{u}_\theta}{\partial x}
\end{aligned} \tag{B-7}$$

hence

$${}^0\dot{\varepsilon}_a = \frac{\partial\,{}^0\dot{u}_x}{\partial x} \;\;;\;\; {}^0\dot{\varepsilon}_\theta = \frac{{}^0\dot{u}_r}{R} \;\;;\;\; {}^0\dot{\varepsilon}_r = \frac{{}^1\dot{u}_r}{R} \;\;;\;\; {}^0\dot{\gamma} = \frac{\partial\,{}^0\dot{u}_\theta}{\partial x} \tag{B-8}$$

Expanding all stress and strain components in (B-2) as indicated in (B-6) the internal virtual work term can be integrated over the wall thickness. The result is

$$\delta W_{\text{int}} = 2\pi R t L\left\{{}^0\sigma_a\,\delta^0\varepsilon_a + {}^0\sigma_\theta\,\delta^0\varepsilon_\theta + {}^0\sigma_r\,\delta^0\varepsilon_r + {}^0\tau\,\delta^0\gamma + O(\xi^2)\right\} \tag{B-9}$$

Note that the first order terms vanish. Expanding the displacements u_j and using (B-8) the external virtual work can be expressed as

$$\begin{aligned}
\delta W_{ext} &= F\,L\,\delta^0\varepsilon_a + M\frac{L}{R}\delta^0\gamma \\
&+ 2\pi R^2 L\left\{p_i\left[\delta^0\varepsilon_\theta - \xi\left(\delta^0\varepsilon_\theta + \delta^0\varepsilon_r\right)\right] - p_e\left[\delta^0\varepsilon_\theta + \xi\left(\delta^0\varepsilon_\theta + \delta^0\varepsilon_r\right)\right] + O(\xi^2)\right\}
\end{aligned} \tag{B-10}$$

Finally, equating internal virtual work (B-9) and external virtual work (B-10), retaining only zero order terms in ξ, yields

$$\begin{aligned}
2\pi R t\;{}^0\sigma_a &= F \\
2\pi R^2 t\;{}^0\tau &= M \\
t\;{}^0\sigma_\theta &= R\,(p_i - p_e) \\
{}^0\sigma_r &= 0
\end{aligned} \tag{B-11}$$

which thin-wall stresses are zero order correct in ξ.

Alternatively, retaining up to the first order ξ terms in equation (B-10) results in

$$\begin{aligned}
2\pi R t\;{}^0\sigma_a &= F \\
2\pi R^2 t\;{}^0\tau &= M \\
t\left({}^0\sigma_\theta - {}^0\sigma_r\right) &= R\,(p_i - p_e) \\
{}^0\sigma_r &= -\frac{1}{2}(p_i + p_e)
\end{aligned} \tag{B-12}$$

and these stresses are first order correct in ξ.

Note that only uniform (zero order) stress terms are involved in equilibrium equations that define stresses correct up to first order. The familiar equations (B-11) are referred to as thin-wall theory; equations (B-12) have been called "3D average" or < 3D > theory.

Appendix C: Yield Collapse

The von Mises yield criterion may be written as

$$\begin{aligned}
&(\sigma_a - \sigma_r)^2 - (\sigma_a - \sigma_r)(\sigma_\theta - \sigma_r) + (\sigma_\theta - \sigma_r)^2 + 3\tau^2 \\
&= \left(\sigma_a - \frac{\sigma_\theta + \sigma_r}{2}\right)^2 + \frac{3}{4}(\sigma_\theta - \sigma_r)^2 + 3\tau^2 = \sigma_y{}^2
\end{aligned} \tag{C-1}$$

Defining "effective axial load" and "effective axial stress" as

$$F_{eff} \equiv 2\pi R t\;\sigma_{a\,eff} = F - \pi R^2\left\{p_i(1-\xi)^2 - p_e(1+\xi)^2\right\} \tag{C-2}$$

the von Mises criterion (C-1) is

$$\left(\sqrt{3}\,\frac{\sigma_\theta - \sigma_r}{2}\right)^2 + \left(\sigma_{a\,eff}\right)^2 + \left(\sqrt{3}\,\tau\right)^2 = \sigma_y{}^2 \tag{C-3}$$

which can be written in terms of loads using equation (B-12)

$$\left(\frac{\Delta p}{\frac{2}{\sqrt{3}}\frac{t}{R}\sigma_y}\right)^2 + \left(\frac{F_{eff}}{2\pi R t\,\sigma_y}\right)^2 + \left(\frac{M}{\frac{2}{\sqrt{3}}\pi R^2 t\,\sigma_y}\right)^2 = 1 \tag{C-4}$$

The effective axial load is a function of both internal and external pressure. Re-organizing equation (C-4) in terms of pressure difference $p_e - p_i$ yields

$$A\left(\frac{\Delta p}{4\xi\sigma_y}\right)^2 + 2B\left(\frac{\Delta p}{4\xi\sigma_y}\right) + C = 0 \tag{C-5}$$

where, defining $S_i = (\sigma_a + p_i)/\sigma_y$ and $T = \tau/\sigma_y$,

$$\begin{aligned}
A &= 3 + (1+\xi)^4 \\
B &= S_i(1+\xi)^2 \\
C &= S_i^2 + 3T^2 - 1
\end{aligned} \tag{C-6}$$

The solution of equation (C-5) is

$$\frac{\Delta p}{2\xi\sigma_y} = \frac{2(1+\xi)^2}{3+(1+\xi)^4}\left[-S_i \pm \sqrt{1 - 3T^2 + 3\,\frac{1 - 3T^2 - S_i^2}{(1+\xi)^4}}\right] \tag{C-7}$$

The equilibrium model (B-12) was first order correct in $\xi = t/(2R)$ for the stresses and therefore equation (C-2) may have been taken linearized as well. In that case equation (C-7) would have been found as

$$\frac{\Delta p}{2\xi\sigma_y} = \frac{2(1+2\xi)}{3+(1+2\xi)^2}\left[-S_i \pm \sqrt{1-3T^2+3\frac{1-3T^2-S_i^2}{(1+2\xi)^2}}\right] \quad \text{(C-8)}$$

Consistent with equations (B-12) the right-hand side of (C-8) is accurate up to first order in ξ and hence may be linearized in ξ resulting in

$$\frac{\Delta p}{2\xi\sigma_y} = -\frac{1}{2}(1+\xi)S_i \pm \left(1-\xi\frac{2-6T^2-3S_i^2}{4-12T^2-3S_i^2}\right)\sqrt{1-3T^2-\frac{3}{4}S_i^2} \quad \text{(C-9)}$$

This linearization brakes down for those load combinations for which the square root factor vanishes (for example at very high axial compression) and in those cases equation (C-8) should be used.

The plus sign in equations (C-7), (C-8) and (C-9) is relevant for almost all of the practical collapse situations where $\Delta p > 0$.

As an alternative for the von Mises yield criterion, the more conservative Tresca criterion may be used. Given the pipe stresses σ_a , σ_θ , σ_r and τ from equation (B-11) the principal stresses are

$$\begin{aligned}\sigma_1 &= \frac{\sigma_a+\sigma_\theta}{2} - \sqrt{\left(\frac{\sigma_\theta-\sigma_a}{2}\right)^2+\tau^2}\\ \sigma_2 &= \frac{\sigma_a+\sigma_\theta}{2} + \sqrt{\left(\frac{\sigma_\theta-\sigma_a}{2}\right)^2+\tau^2}\\ \sigma_3 &= \sigma_r\end{aligned} \quad \text{(C-10)}$$

The Tresca yield criterion is

$$\max\left\{|\sigma_1-\sigma_2| \ , \ |\sigma_2-\sigma_3| \ , \ |\sigma_3-\sigma_1|\right\} = \sigma_y \quad \text{(C-11)}$$

Yield Collapse – External Pressure only

If only external pressure is present, $S_i = 0$ and $T = 0$ and then equation (C-9) becomes simply

$$p_e^{yc} = 2\sigma_y\ \xi\left(1-\frac{1}{2}\xi\right) \quad \text{(C-12)}$$

In Fig. C.1 this formula is compared with the formula by Tamano *et al.*[1]

$$p_e^{ycT} = 2\sigma_y\ \frac{D/t-1}{(D/t)^2}\left(1+\frac{fac}{D/t-1}\right) \quad \text{(C-13)}$$

and with the exact through-wall yield solution found by integrating from the inside radius r_i to the outside radius r_e

$$\frac{d\sigma_r}{dr} = \frac{-1}{2r}\left(\sigma_r+\sqrt{4\sigma_y^2-3\sigma_r^2}\right) \ ; \quad p_e = -\sigma_r\big|_{r=r_e} \quad \text{(C-14)}$$

Note that both equations (C-12) and (C-13) are second order correct in ξ, provided $fac = 1.5$. In that case

$$p_e^{yc} = 2\sigma_y\ \xi\left(1-\frac{1}{2}\xi\right) \cong p_e^{ycT} = 2\sigma_y\ \frac{t}{D}\left(1+\frac{1}{2}\frac{t}{D}\right) \quad \text{(C-15)}$$

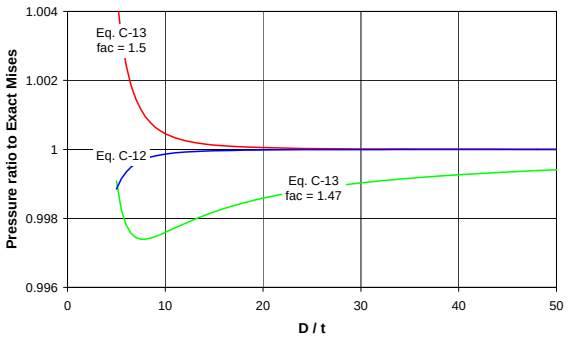

Fig. C.1 Accuracy of the various through-wall yield formulas

Yield Collapse – API 5C3 Approach to Combined Loads

It may be interesting to compare the combined loading collapse equation (8) to the API 5C3 approach[2] to combined loading. Within the context of the new model presented here but following the logic given in API 5C3, one would use the elastic collapse equation (1) for only external pressure

$$p_e^{ec} = \frac{2E'}{1-\nu^2}\ \xi^3\ (1+c\xi) \quad \text{(C-16)}$$

and the yield equation (4) for only external pressure based on the "axial stress equivalent yield strength" to account for axial load

$$p_e^{yc} = 2\xi\sigma_y'\left(1-\frac{1}{2}\xi\right)\left[\sqrt{1-\frac{3}{4}\left(\frac{\sigma_a}{\sigma_y'}\right)^2}-\frac{1}{2}\frac{\sigma_a}{\sigma_y'}\right] \quad \text{(C-17)}$$

Solving for the external collapse pressure using (C-16) and (C-17) in equation (8) :

$$\hat{p}_e^c = \frac{2\ p_e^{yc}\ p_e^{ec}}{p_e^{yc}+p_e^{ec}+\sqrt{\left(p_e^{yc}-p_e^{ec}\right)^2+4H_t\ p_e^{yc}\ p_e^{ec}}} \quad \text{(C-18)}$$

Finally, introducing the "external pressure equivalent" to account for internal pressure, the result would be

$$p_e^c = \hat{p}_e^c + \left(1-2\frac{t}{D}\right)p_i \quad \text{(C-19)}$$

Appendix D: API 5C3 Average Collapse

API Bulletin 5C3[2] provides not only the formulas for the lower bound design values for collapse strength. The document also describes the formulas for average collapse. The basis for these formulas is the regression equation fitting 2488 tests, called plastic collapse. That formula for plastic collapse was augmented with a yield collapse formula and an elastic collapse formula. The yield collapse formula was conservatively taken as the external pressure that generates minimum yield stress on the inside wall of the pipe calculated by means of the Lamé equations. The elastic collapse pressure formula was derived from the formula developed by Clinedinst[4]: the average elastic collapse resistance was taken as 95 percent of that formula.

The "axial stress equivalent yield strength" is defined as

$$\sigma_{ya} = \sigma_y \left[\sqrt{1 - \frac{3}{4}\left(\frac{\sigma_a}{\sigma_y}\right)^2} - \frac{1}{2}\frac{\sigma_a}{\sigma_y} \right] \quad \text{(D-1)}$$

Two constants *A* and *B* are

$$A = 2.8762 + \frac{\sigma_{ya}}{100}\left(0.10679 + \frac{\sigma_{ya}}{100}\left(0.21301 - \frac{\sigma_{ya}}{100}0.053132\right)\right) \quad \text{(D-2)}$$

$$B = 0.026233 + \frac{\sigma_{ya}}{100}\,0.050609 \quad \text{(D-3)}$$

where the yield strength σ_{ya} is to be taken as its value in [ksi]. The API 5C3 average *yield* collapse pressure in [ksi] is

$$p^{ycA} = 2\sigma_{ya}\frac{D/t - 1}{(D/t)^2} \quad \text{(D-4)}$$

the API 5C3 average *plastic* collapse pressure in [ksi] is

$$p^{pcA} = \sigma_{ya}\left(\frac{A}{D/t} - B\right) \quad \text{(D-5)}$$

and the API 5C3 average *elastic* collapse pressure in [ksi] is

$$p^{ecA} = 62600\,\frac{1}{D/t(D/t - 1)^2} \quad \text{(D-6)}$$

Which of the three formulas (D-4), (D-5) or (D-6) governs, is determined by the *D/t* ratio and the yield strength σ_{ya} according to the following decision scheme:

$$\begin{aligned}
&\textit{if} \quad \frac{D}{t} < \frac{\sqrt{(A-2)^2 + 8B} + A - 2}{2B} \quad \textit{then} \\
&p_e^{cA} = p^{ycA} + \left(1 - 2\frac{t}{D}\right) p_i \\
&\textit{elseif} \quad p^{ecA} < p^{ycA} \quad \textit{or} \quad \frac{D}{t} > \frac{2 + B/A}{3B/A} \quad \textit{then} \\
&p_e^{cA} = p^{ecA} + \left(1 - 2\frac{t}{D}\right) p_i \\
&\textit{else} \\
&p_e^{cA} = p^{pcA} + \left(1 - 2\frac{t}{D}\right) p_i
\end{aligned} \quad \text{(D-7)}$$

This logic scheme defines the average external collapse pressure p_e^{cA} in units [ksi] under combined axial stress σ_a in [ksi] and internal pressure p_i in [ksi].